17th Brazilian Congress of Thermal Sciences and Engineering
November 25th-28th, 2018, Águas de Lindóia, SP, Brazil

ENCIT-2018-0460
ASSESSMENT OF AIRFOILS FOR A UAV FOR PULVERIZATION APPLICATION

João Carlos Teles Ribeiro da Silva
Federal Institute of South of Minas Gerais - IFSULDEMINAS, Road from Muzambinho to Nova Resende, km 35, Bairro Morro Preto, Muzambinho, Minas Gerais, 37890-000, Brazil.
joao.silva@muz.ifsuldeminas.edu.br

Kamal Abdel Radi Ismail
Faculty of Mechanical Engineering of the University of Campinas - FEM/UNICAMP, Department of Thermal and Fluid Engineering, Mendeleyev Street, 200, University City "Zeferino Vaz", Barão Geraldo, Campinas, São Paulo, 13083-860, Brazil.
kamal@fem.unicamp.br

Abstract. *The purpose of this work is evaluated different airfoils and their suitability in the project of a wing for the aerial agricultural pulverization application. The aerodynamic profiles chosen were NACA 4415, NACA 65-210, GOE 244 and J 0513, respectively characterized as: commercial, laminar flow, high lift and analytical. The aerodynamic analysis was performed through computational routines using a three dimensional panel method. The results were presented, compared and discussed. The relevance of this work is in the proper choice of aspect ratio and in the appropriate selection of the airfoil that composes the wing, considering the operating conditions of the aircraft's mission. The most suitable airfoil was NACA 65-210 applied to a wing with the aspect ratio 5.*

Keywords: *aerodynamics, laminar flow airfoil, pesticides, wing design*

1. INTRODUCTION

The UAVs (Unmanned Aerial Vehicles) have many applications in agriculture and livestock farming business. In this way, the present work aimed the wing aerodynamic design for a UAV suitable for the agrochemicals application. Therefore, the NACA 4415 (commercial airfoil), NACA 65-210 (laminar flow airfoil), the Göttingen GOE 244 (high lift airfoil) and the Kutta-Joukowski J 0513 (analytical airfoil) were compared.

Recently, Matsuo and Ismail (2010) performed the optimization of the aerodynamic profile NACA 4415 for a UAV with agricultural application, concluding than this optimization for the N1PVA profile was satisfactory, allowing a better performance of the aircraft in takeoff and also an increase of its payload. The choice of profile to be optimized was due to its extensive use in manned agricultural aircraft.

Currently, the efficiency in the application of agricultural pesticides is minimal and alarming. The percentage distribution of pesticides in the bean crop was evaluated by Chaim (2017), who indicates the loss in the current scenario, since little was changed in the machines for this application, and it was concluded that 77% of the total that is applied is loss, and only the remaining 23% reach the selected target (the plant, in this case), being part of the drift loss and evaporation loss (59%), and the soil loss (18%).

A recent study based on the influence of aerodynamic coefficients on integrated flexible dynamic load models was carried out using the tridimensional panels method, and concluded that the method has a great potential to improve the accuracy and precision in the simulation of maneuvers and gusts loads, as well as for calculating the aeroelastic resonance effect (flutter, also known as the "wing-break" effect). This allows fast determination of the maneuvers and gusts envelope for the aircraft design (Kier *et al.*, 2015).

The dipole lattice method was developed through software based panel method, available as open source. This application is used to obtain the basic unsteady aerodynamics model of a flexible unmanned air vehicle with a body freedom flutter. The software was promising, being an opportunity for the scientific community to compare among its analysis techniques (Kotikalpudi *et al.*, 2015).

The combination of experimental wind tunnel test values with the panel method can attend the development of the aerodynamic configuration design for solar powered buoyancy-lifting unmanned aerial vehicle in the near-space resulting in an adequate relationship between lift and drag that was validated with experimental data (Chen *et al.*, 2015).

The ducted propellers, intended for naval application, were designed from the potential flow modeling using the panel method. The analysis is performed for the Ka4-70 propeller operating within the duct 19A. Numerical results are compared with experimental data available from open water tests. A large variation in force calculations was found due to the thickness of the boundary layer in the duct. For this, a careful tuning was necessary to correctly predict the

characteristics in open water, concluding that the panel method provided an acceptable prediction of these characteristics (Baltazar *et al.*, 2015).

Lastly, the panel method is widely used by the scientific community to determinate the aerodynamics coefficients.

2. METHODOLOGY

The panel method (Baltazar *et al.*, 2015; Kier et al., 2015; Kotikalpudi *et al.*, 2015) was used to calculate the aerodynamic coefficients to the four airfoils. Some basic definitions are important and they are presented below.

Firstly, Tab. 1 presents zero lift angle of attack (α_{L0}), stall angle of attack (α_{stall}), maximum coefficient of lift ($c_{l,\,max}$), lift-curve slope for airfoil (a_0) and profile coefficient of drag (c_d).

Table 1. Airfoils characteristics (Anderson Jr., 2015; Ismail, 2009).

Characteristics	NACA 4415	NACA 65-210	GOE 244	J 0513
α_{L0} [(1)]	-4.1000	-2.0000	-12.500	-5.8000
α_{stall} [(1)]	12.000	10.700	10.200	11.050
$c_{l,\,max}$	1.4000	1.2700	1.9205	1.5957
c_d	0.0078	0.0045	0.0170	0.0090
a_0	5.9683	5.7296	5.6746	6.2063

(1) (deg).

Due to the downwash effect, the angles of attack (AoA) as geometric angle of attack (α_{geom}), effective angle of attack (α_{eff}) and induced angle of attack (α_i) are given by:

$$\alpha_{geom} = \alpha_{eff} + \alpha_i \tag{1}$$

Tip chord (c_t) is taper ratio (λ) multiplied by root chord (c_r). However, wing area (S) is given by (being that *s*, typed in lowercase, means half-wingspan):

$$S = (c_r + c_t)s \tag{2}$$

Mean aerodynamic chord, $\overline{c}$, is given by:

$$\overline{c} = \frac{2}{3} c_r \frac{1 + \lambda + \lambda^2}{1 + \lambda} \tag{3}$$

Aspect ratio, A, is given by:

$$A = \frac{4s^2}{S} \tag{4}$$

Air is characterized by freestream fluid cinematic viscosity (ν_∞, air at 1100 m upper sea level and 15 °C is 1.5111×10^{-5} $m^2.s^{-1}$) and freestream fluid density (ρ_∞, air at 1100 m upper sea level and 15 °C is 1.1008 $kg.m^{-3}$). Velocity of the body through the fluid, or freestream velocity of the fluid (V_∞) is given by (being that Re is the Reynolds number):

$$V_\infty = \frac{\nu_\infty Re}{\overline{c}} \tag{5}$$

Coefficient of lift, C_L, is given by (being that W means wing load):

$$C_L = \frac{2W}{\rho_\infty {V_\infty}^2 S} \tag{6}$$

Coefficient of induced drag, $C_{D,i}$, is given by (being that e is the Oswald factor):

$$C_{D,i} = \frac{{C_L}^2}{\pi e A} \tag{7}$$

Pressure coefficient, C_p, is given by the difference between static pressure (p) at the point at which C_p is being evaluated and static pressure in the freestream (p_∞), it followed by the division by the dynamic pressure:

$$C_p = \frac{p - p_\infty}{\frac{1}{2}\rho_\infty {V_\infty}^2} \tag{8}$$

After all, the dimensionless parameter of the wing's pitching moment coefficient, C_m, is defined as:

$$C_m = \frac{Moment}{\frac{1}{2}\rho_\infty {V_\infty}^2 S l} \tag{9}$$

where l is the lever arm length. Aircraft horizontal tail sizing according to stability requirement. The pitch moment coefficient, over an AoA, is responsible for the stability of the aircraft around the lateral axis.

3. RESULTS

This topic shows the results based on the panel method. In all cases, the wing load was 150 kg.

Table 2. The four wings AoA.

AoA	NACA 4415	NACA 65-210	GOE 244	J 0513
α_i [(1)]	1.18	1.18	3.68	2.65
α_{eff} [(1)]	-1.01	1.20	-2.43	0.83
α_{geom} [(1)]	0.17	2.38	1.24	3.48

(1) (deg).

Table 3. Numerical results of the four wings.

Characteristics	NACA 4415	NACA 65-210	GOE 244	J 0513
α_{geom} [(1)]	0.17	2.38	1.24	3.48
V_∞ [(2)]	33.8	36.4	20.2	23.8
C_L	0.3240	0.2793	0.9096	0.6552
$C_{D,\,i}$	0.0066	0.0049	0.0517	0.0269
L/D	49.454	57.447	17.582	24.401
C_m	-0.1757	-0.1124	-0.4765	-0.3119
x_{CP} [(3)]	1092.3	928.8	1070.8	1010.4

(1) (deg). (2) (m.s^{-1}). (3) (mm).

Analyzing Fig. 1 and Fig. 2, and especially the values in Tab. 3, it can be seen that the NACA 65-210 wing shows a better result in the values of L/D and C_m in relation to the NACA 4415 wing. That is, the NACA 65-210 wing compared to NACA 4415 wing has advantages: 26% lower $C_{D,\,i}$, 36% lower C_m and 16% higher L/D. As disadvantages, the NACA 65-210 wing presents in relation to the NACA 4415 wing: 14% lower C_L and 8% higher cruising speed. Thus, it can be concluded that the NACA 65-210 wing presents a more adequate aerodynamic efficiency for the case.

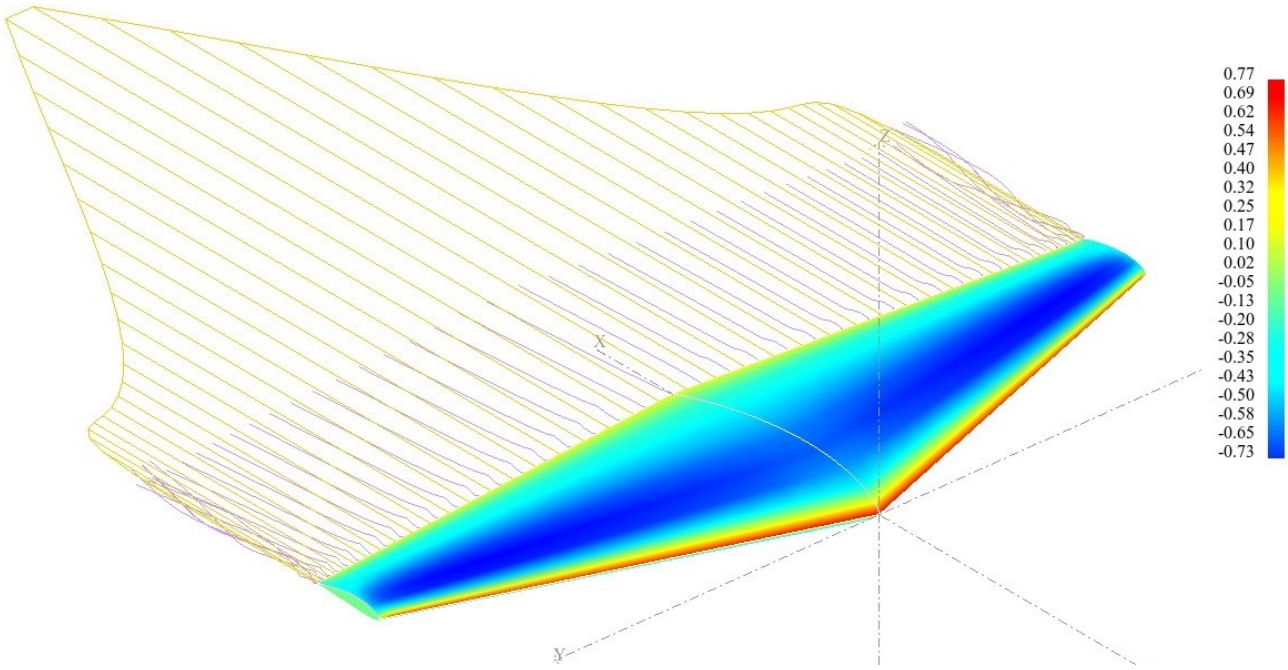

Figure 1. C_p for NACA 4415, λ = 0.3, AR = 4.99, c_r = 1.85 m e s = 3 m.

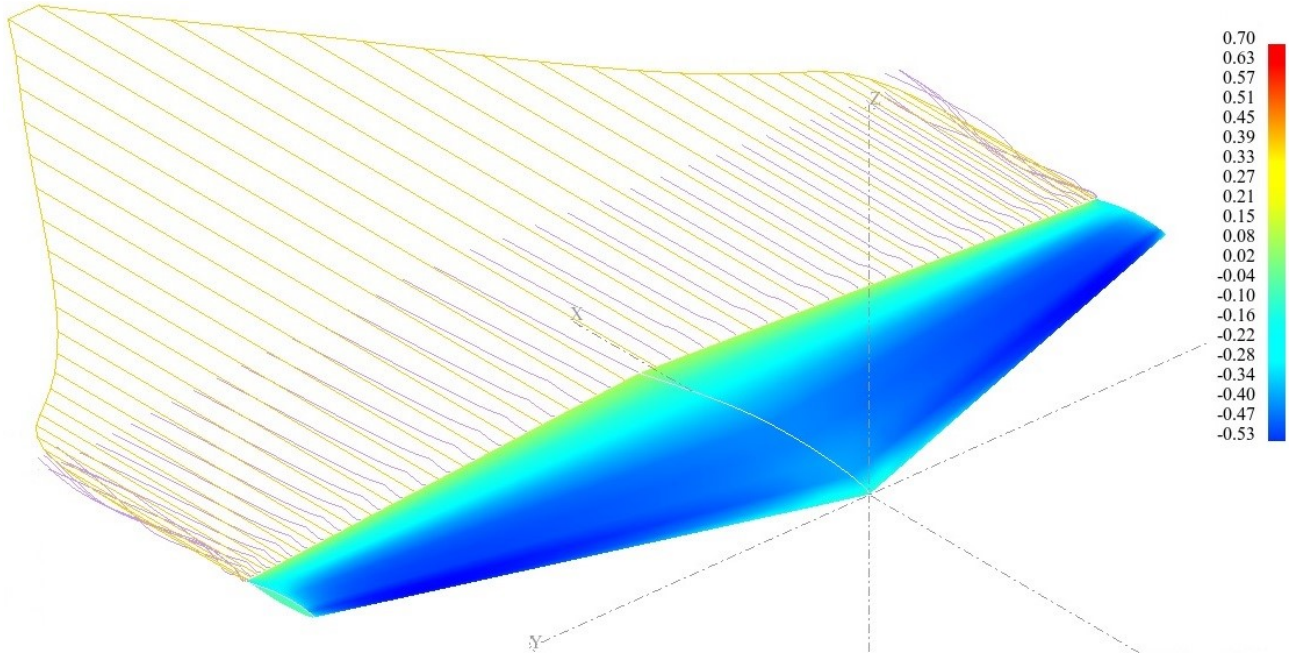

Figure 2. C_p for NACA 65-210, λ = 0.3, AR = 4.99, c_r = 1.85 m e s = 3 m.

The NACA 65-210 wing was the basis of comparison for the other two wings. After that, when Fig. 3 compared to Fig. 2, and observing the values of Tab. 3, it is found that the GOE 244 wing presents disadvantages in relation to the NACA 65-210 wing: 955% higher $C_{D,\ i}$, 324% higher C_m and 69% lower L/D. As an advantage, the GOE 244 wing presents in relation to the NACA 65-210 wing: 226% higher C_L and 45% lower cruising speed.

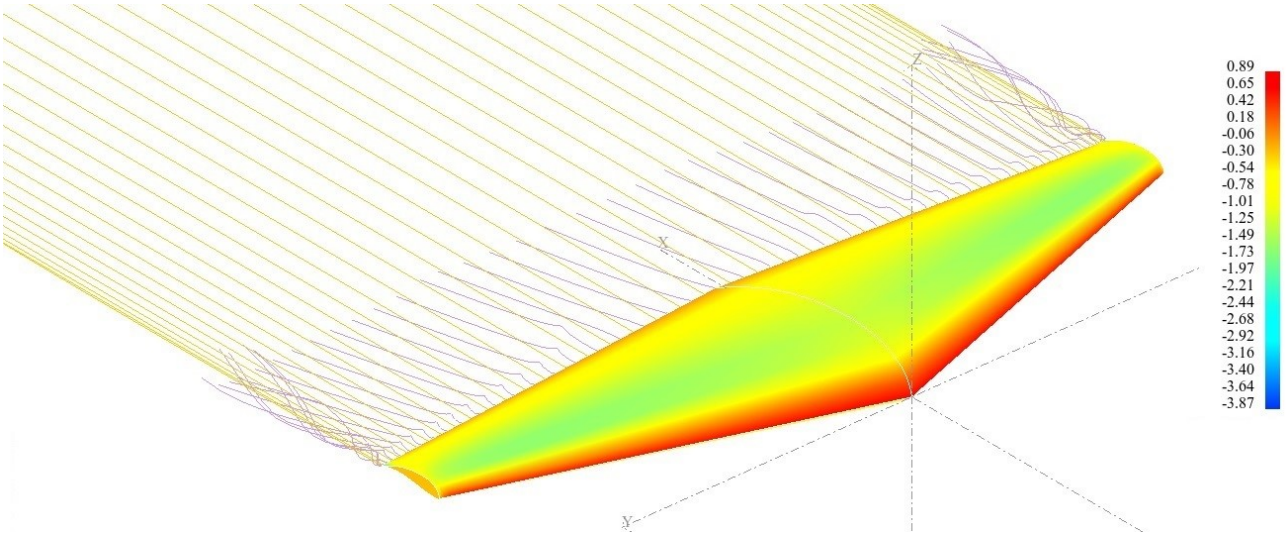

Figure 3. C_p for GOE 244, $\lambda = 0.3$, $AR = 4.99$, $c_r = 1.85$ m e $s = 3$ m.

When Fig. 4 compared to Fig. 2, and the values of Tab. 3, it is found that the J 0513 wing presents disadvantages in relation to the NACA 65-210 wing: 449% higher $C_{D,\,i}$, 177% higher C_m and 57% lower L/D. As an advantage, the J 0513 wing presents in relation to the NACA 65-210 wing: 135% higher C_L and 35% lower cruising speed.

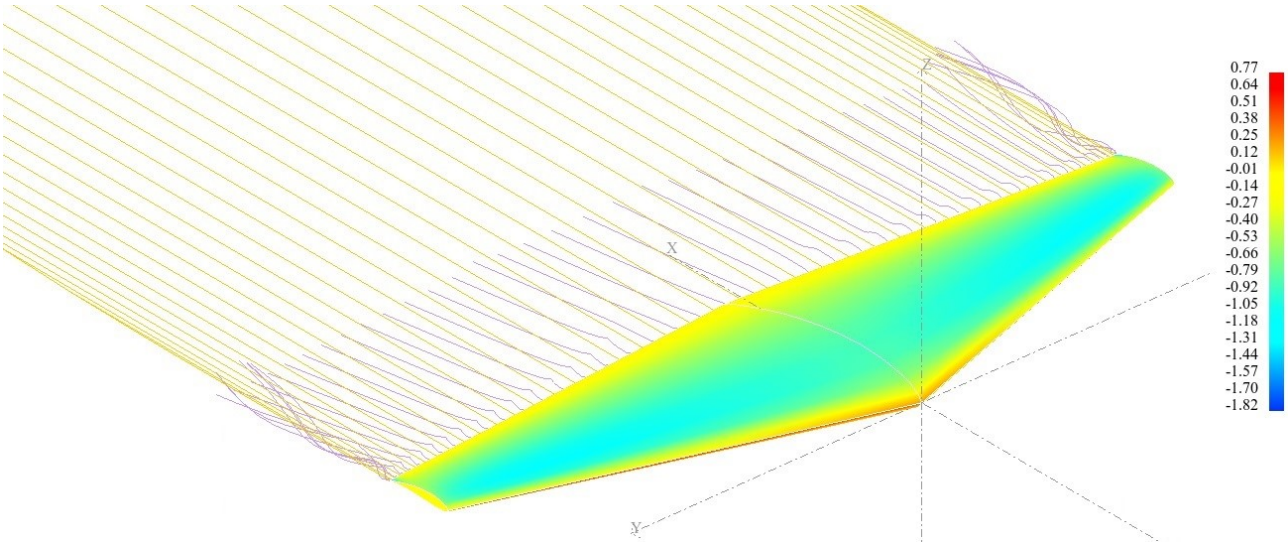

Figure 4. C_p for J 0513, $\lambda = 0.3$, $AR = 4.99$, $c_r = 1.85$ m e $s = 3$ m.

Figure 5 shows that the NACA 65-210 wing is more suitable than the three others in the continuity and uniformity of the distribution of the pressure field around the set of airfoils and the deltas of pressure between the upper and lower surface to the same relative position to the chord. The discontinuities in the distribution found for the three other wings result in higher losses, a greater intensity of aerodynamic noise, a greater propensity to the airflow separation and a greater tendency to form shock waves at higher operational speeds, even for Mach value up to 1.

Therefore, the NACA 65-210 profile presents a better result in aerodynamic efficiency and wing pitch momentum coefficient resulting in the following final characteristics: wingspan of 6 m, root chord of 1.85 m, taper ratio of 0.3, operational speed of 34.4 m.s^{-1}, stall speed of 20.2 m.s^{-1} and geometric angle of attack of 2.38°. It is important to mention that the results obtained were satisfactory for the proposed aero-agricultural pulverization UAV.

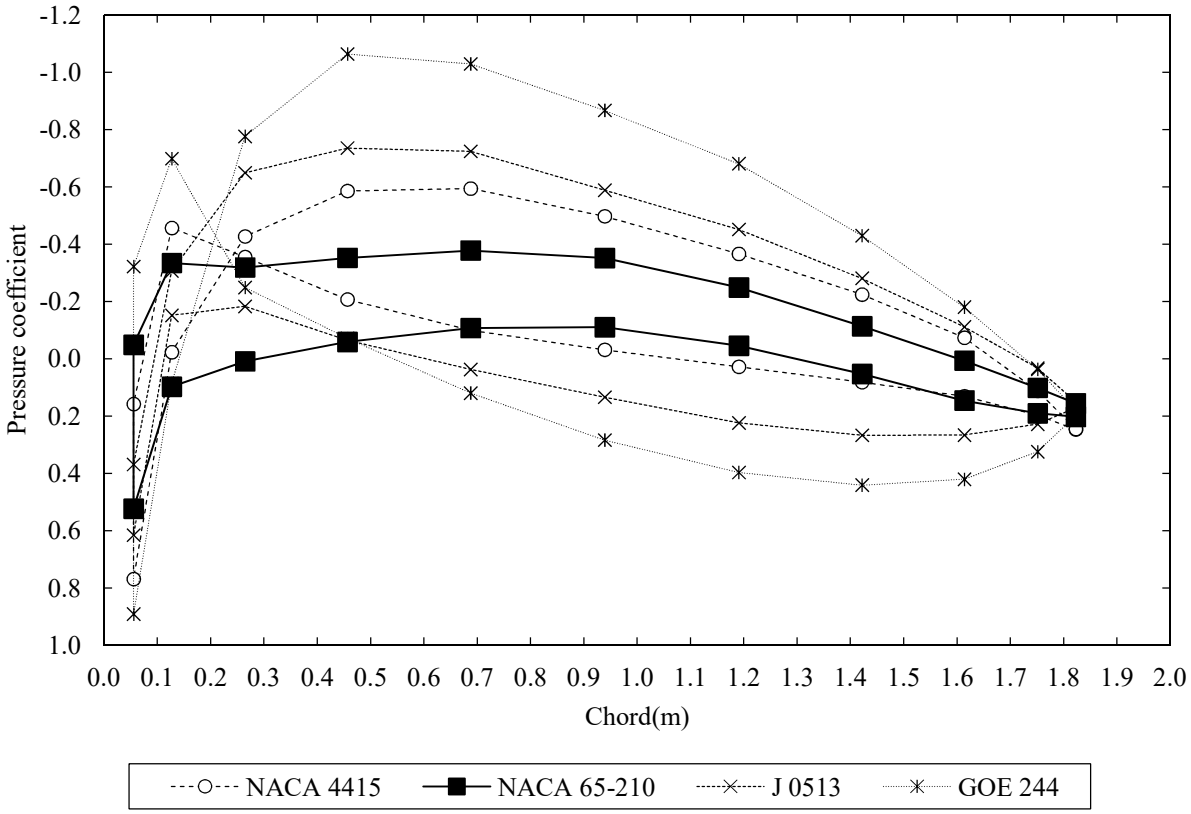

Figure 5. Distribution of C_p to the four wings.

4. CONCLUSIONS

Four aerodynamic profiles were evaluated for the wing's proposed parameters, which allowed the designer to define important performance characteristics of the future aircraft from the point of maximum aerodynamic efficiency. Finally, the NACA 65-210 laminar flow profile was more suitable for the application and construction of the aero-agricultural pulverization UAV wing.

5. REFERENCES

Anderson Jr., J.D., 2015. *Fundamentos de engenharia aeronáutica: introdução ao voo*. McGraw-Hill, Porto Alegre, 7th edition.

Baltazar, J., Falcao de Campos, J.A.C. and Bosschers, J., 2015. "Potential flow modelling of ducted propellers with a panel method". In *Proceedings of the Fourth International Symposium on Marine Propulsors*. Austin, Texas, USA.

Chaim, A., 2017. "Eficiência de aplicação". Embrapa de Informação Tecnológica. 9 Jun. 2017 <http://www.agencia.cnptia.embrapa.br/gestor/agricultura_e_meio_ambiente/arvore/CONTAG01_44_210200792814.html>

Chen, G., Chen, B., Li, P., Bai, P. and Ji, C., 2015. "Study of aerodynamic configuration design and wind tunnel test for solar powered buoyancy-lifting vehicle in the near-space". *Procedia Engineering*, Vol. 99, p. 67-72.

Ismail, K.A.R., 2009. *Aerodinâmica básica*. Author's Publisher, Campinas, 2nd edition.

Kier, T., Verveld, M.J. and Burkett, C.W., 2015. "Integrated Flexible Dynamic Loads Models Based on Aerodynamic Influence Coefficients of a 3D Panel Method". In *International Forum on Aeroelasticity and Structural Dynamics - IFASD2015*. Saint Petersburg, Russia. (p. 179).

Kotikalpudi, A., Pfifer, H. and Balas, G.J., 2015. "Unsteady aerodynamics modeling for a flexible unmanned air vehicle". In *AIAA Atmospheric Flight Mechanics Conference - AFM2015*. Reston, USA. (p. 2854).

Matsuo, C.A.S., Ismail, K.A.R., 2010. "Otimização do aerofólio NACA para um veículo aéreo não tripulado com aplicação agrícola," *Mecánica Computacional*, Vol. 29, p. 3657-3669.

6. RESPONSIBILITY NOTICE

The authors are the only responsible for the printed material included in this paper.